

# Isoscalar Giant Resonances in Calcium Isotopes Using CDFT and Finite Amplitude Method

**M. El Adri, Y. El Bassem, A. El Batoul, M. Oulne**

High Energy Physics and Astrophysics Laboratory, Department of Physics,  
Faculty of Sciences Semlalia, Cadi Ayyad University, P.O.B. 2390,  
Marrakesh, Morocco

**Abstract.** Using the quasiparticle finite amplitude method within covariant density functional theory and the DD-ME2 density-dependent meson-exchange model, we study isoscalar giant monopole and quadrupole resonances in calcium isotopes. Numerical implementation is examined for  $^{40-44}\text{Ca}$  and  $^{48}\text{Ca}$ , showing good agreement with available experimental isoscalar giant monopole strengths. In the neutron-deficient isotopes  $^{30-38}\text{Ca}$ , and in exotic region  $^{56-60}\text{Ca}$ , we identify the well-known monopole-quadrupole coupling that splits the isoscalar giant monopole resonance.

## 1 Introduction

The study of the isoscalar giant resonance [1, 2], particularly its monopole component, remains essential for advancing our understanding of nuclear forces and connecting nuclear physics with astrophysics. This collective excitation provides vital information about the properties of nuclear matter under extreme conditions and plays a key role in determining nuclear incompressibility, a crucial parameter in the nuclear equation of state. Furthermore, examining this resonance helps validate theoretical models and offers insights into astrophysical phenomena such as neutron star structure and nuclear symmetry energy.

The isovector giant dipole resonance (IVGDR) was initially discovered in 1947 through various methods including photoabsorption, inelastic scattering, and  $\gamma$ -decay [3, 4]. The isoscalar giant quadrupole resonance (ISGQR) was subsequently observed between 1971 and 1972 [5, 6], with the isoscalar giant monopole resonance (ISGMR) being identified later in 1977 [7]. Analysis of experimental data has led to the establishment of empirical formulas describing the energies of these resonances [8, 9]. Among them, the ISGMR is particularly important because of its connection to the nuclear incompressibility coefficient  $K_0$  [10, 11]. Building on this foundation, the present study investigates nuclear excitation properties through microscopic methods, mainly the Generator Coordinate Method (GCM) and the Random Phase Approximation (RPA). While GCM combines Hartree-Fock-Bogoliubov states, RPA provides a computation-

ally efficient framework that accounts for particle-hole excitations. Originating in condensed matter physics and later adapted to nuclear systems, RPA has evolved into more sophisticated forms such as QRPA and the Finite Amplitude Method, enhancing its applicability to nuclear resonance phenomena.

This research focuses on calcium isotopes, which are well suited to examining complex nuclear phenomena due to their structural properties and magicity features. It explores resonances in the isoscalar monopole strength distribution, taking into account the impact of neutron excess. Experimental data reveal enhanced monopole strength across various nuclear regions, with some resonances attributed to isoscalar monopole-quadrupole coupling. To analyse these features, the study uses relativistic mean field calculations to determine ground state properties, and the finite amplitude quasiparticle method (QFAM) to study isoscalar giant monopole and quadrupole resonances in calcium isotopes. The organization of this paper is as follows: Section 2 offers a concise overview of the methods used in our calculations. In Section 3, we detail the numerical procedures, describe the interactions applied, and present a thorough analysis and discussion of the results. Finally, Section 4 summarizes the key conclusions derived from our study.

## 2 Theoretical framework

The Relativistic Hartree-Bogoliubov (RHB) framework is a powerful approach for investigating the structural properties, decay modes, and excited states of both spherical and deformed nuclei. Within this formalism, the nuclear state is represented by a generalized Slater determinant  $|\Phi\rangle$ , serving as a vacuum for independent quasiparticles. These quasiparticles are introduced through a unitary Bogoliubov transformation, from which the Hartree-Bogoliubov wave functions,  $U$  and  $V$ , are obtained as solutions of the RHB equation :

$$\begin{pmatrix} h_D - m - \lambda & \Delta \\ -\Delta^* & -h_D^* + m + \lambda \end{pmatrix} \begin{pmatrix} U_k \\ V_k \end{pmatrix} = E_k \begin{pmatrix} U_k \\ V_k \end{pmatrix}. \quad (1)$$

In this equation, the operator  $h_D$  designates the single-nucleon Dirac Hamiltonian, whereas  $\Delta$  denotes the pairing field, with  $U$  and  $V$  corresponding to the Dirac spinors.

The quasiparticle finite amplitude method (QFAM) is formulated on the basis of the linear response equations [12], which establish the theoretical framework for investigating the dynamical response of the nuclear system under external perturbations

$$(E_\mu + E_\nu - \omega) X_{\mu\nu}(\omega) + \delta H_{\mu\nu}^{20}(\omega) = -F_{\mu\nu}^{20}, \quad (2)$$

$$(E_\mu + E_\nu + \omega) Y_{\mu\nu}(\omega) + \delta H_{\mu\nu}^{02}(\omega) = -F_{\mu\nu}^{02}, \quad (3)$$

In this expression,  $E_\mu$  and  $E_\nu$  denote the quasiparticle energies, while  $X_{\mu\nu}$  and  $Y_{\mu\nu}$  represent the transition amplitudes. Specifically,  $\mu\nu$  corresponds to the

annihilation of two quasiparticles labeled as '02', and  $\mu\nu$  refers to the creation of two quasiparticles labeled as '20'. The term  $\delta H$  signifies the induced Hamiltonian resulting from the perturbation of the nuclear system by an external field  $F$  at a frequency  $\omega$ . Within this framework, the dynamical response of the system to external excitations can be systematically investigated, thereby providing deeper insights into its collective modes and excitation mechanisms. Finally, the response function can be expressed as follows:

$$S_F(\hat{F}, \omega) = -\frac{1}{\pi} \text{Im} \sum_{\mu\nu} F_{\mu\nu}^{20*} X_{\mu\nu}(\omega) + F_{\mu\nu}^{02*} Y_{\mu\nu}(\omega), \quad (4)$$

The quasiparticle finite amplitude method (QFAM) calculations were performed within the Relativistic Hartree-Bogoliubov (RHB) framework, allowing for a systematic study of the evolution of monopole resonances as a function of neutron excess, and linking this evolution to their coupling with quadrupole resonances.

### 3 Results and discussion

The present study adopts the numerical approach described in Refs. [13, 14], using a fully anisotropic axially deformed harmonic oscillator basis with  $N_F = 12$  shells for fermions and  $N_B = 20$  shells for bosons. Within this basis, the RHB equations together with the nucleon equations of motion are solved self-consistently using the covariant density-dependent meson-exchange functional DD-ME2 [15]. Pairing correlations in open-shell nuclei are treated with the separable pairing interaction introduced by Tian et al. [16], implemented in coordinate space. Furthermore, a smearing parameter of  $\gamma/2 = 1.5$  MeV is adopted to account for the spreading width of the excitations.

The isoscalar giant monopole resonances (ISGMR) for  $^{40-60}\text{Ca}$  isotopes have been systematically calculated using the Quasiparticle Finite Amplitude Method (QFAM) within the covariant density functional theory framework. These calculations, presented in Figure 2, provide comprehensive strength distributions and are directly compared with available experimental measurements for the stable isotopes  $^{40-44,48}\text{Ca}$ . The theoretical analysis covers an extended frequency range up to 35 MeV with a fine energy resolution step of 0.25 MeV, ensuring accurate reproduction of both the main resonance peak and any fragmentation structure. The theoretical predictions show good agreement with experimental data. For the doubly magic  $^{40}\text{Ca}$  nucleus, the calculated ISGMR centroid energy shows remarkable precision with deviations of less than 1.5 MeV from experimental values, validating the theoretical framework where shell effects are most pronounced. The agreement remains acceptable for  $^{42}\text{Ca}$  with deviations below 3 MeV, despite the added complexity of unpaired neutrons beyond the  $N = 20$  shell closure. Similarly,  $^{42}\text{Ca}$  maintains good theoretical-experimen-

*Isoscalar Giant Resonances in Calcium Isotopes using CDFT and ...*

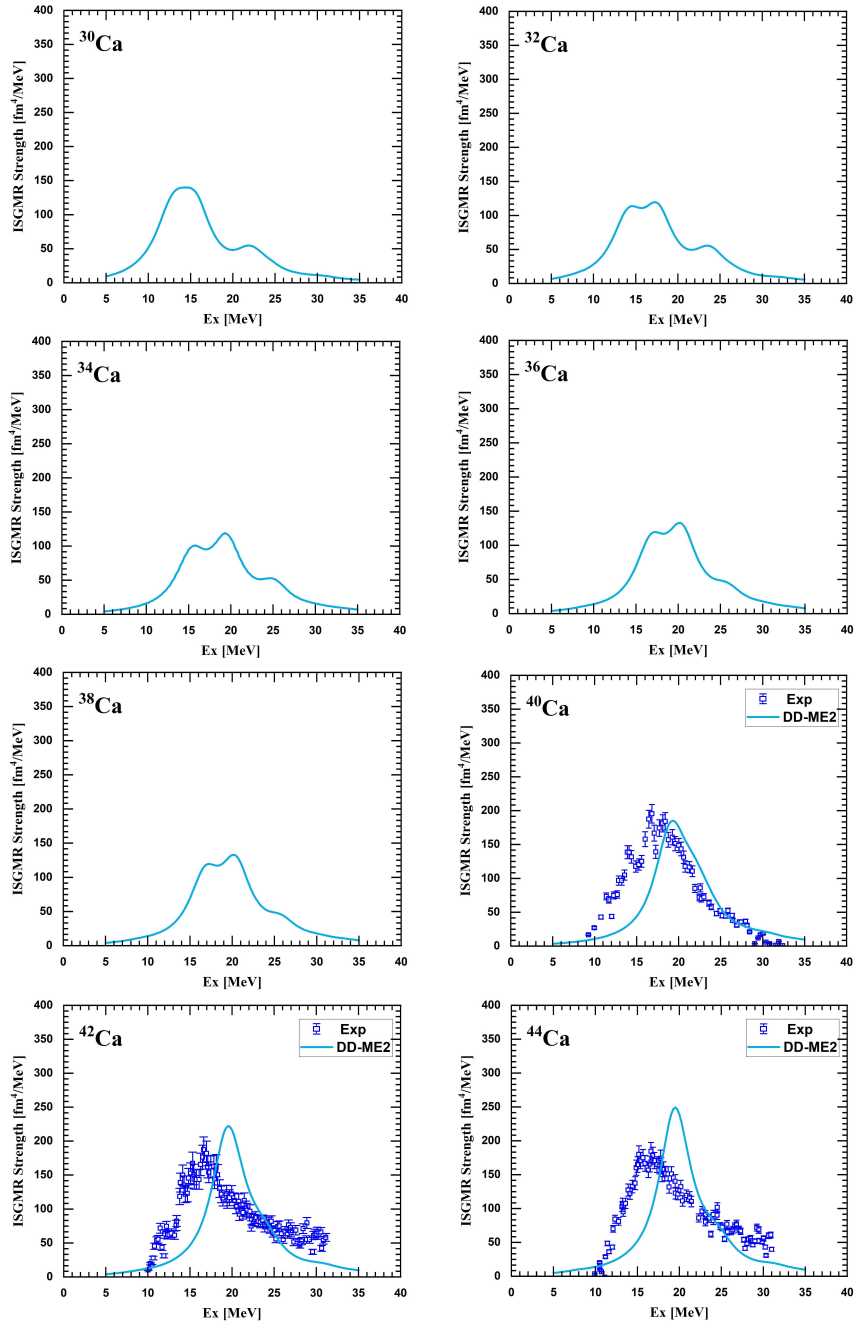


Figure 1. continued on the next page.

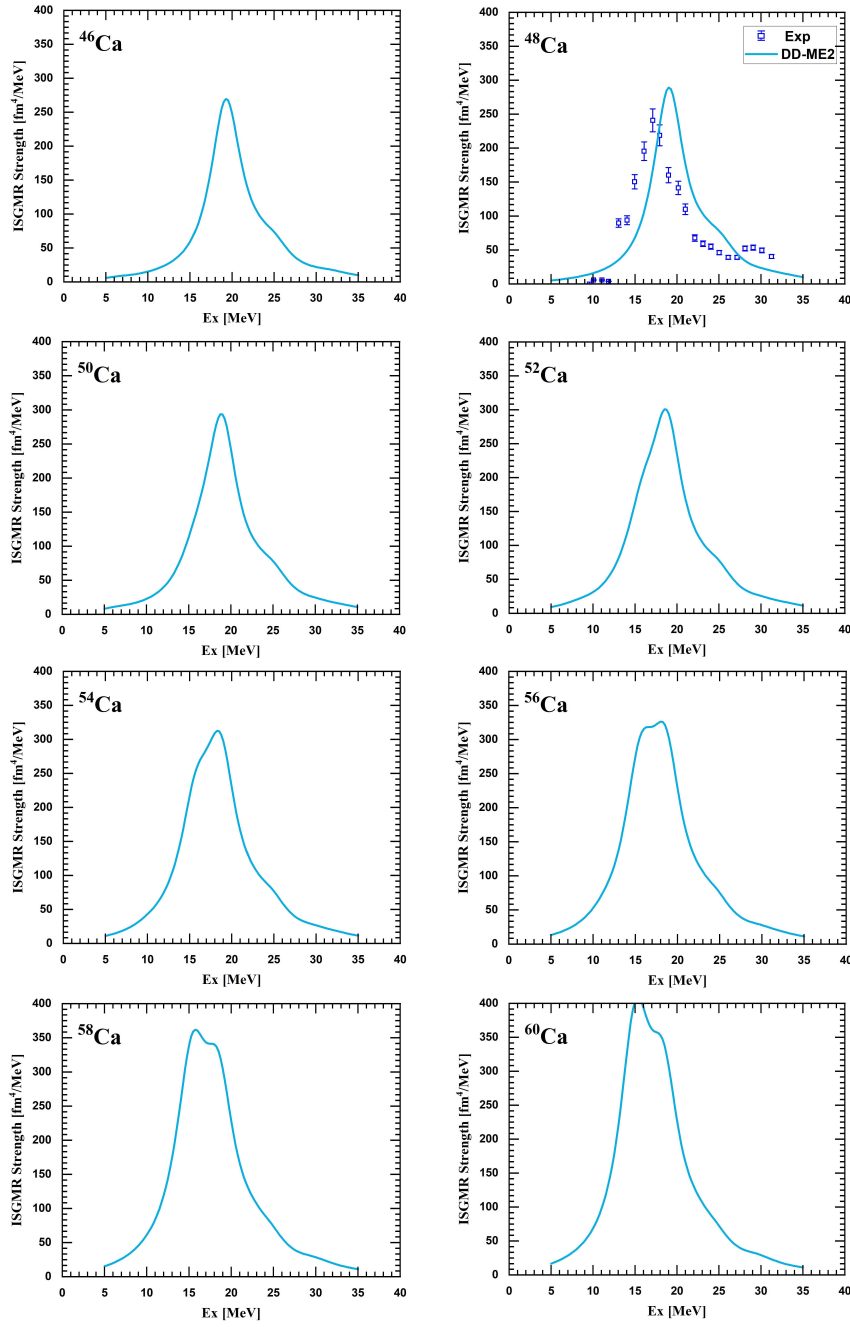


Figure 1. The calculated isoscalar monopole strengths in some Mo isotopes, within DD-ME2 model. The strengths are compared with the available experimental data.

tal consistency with deviations less than 3 MeV, while the semi-magic  $^{42}\text{Ca}$  ( $N = 28$ ) exhibits particularly strong agreement with deviations under 2 MeV.

For the neutron-deficient  $^{30}\text{Ca}$ , we observe a characteristic two-peak structure with a dominant low-energy peak at approximately 14 MeV and a prominent high-energy shoulder around 23 MeV, indicating significant prolate deformation. As neutrons are added progressing through  $^{32}\text{Ca}$ ,  $^{34}\text{Ca}$  and neighboring isotopes, the main peak undergoes splitting into two components, with the primary peak systematically shifting toward higher energies while the high-energy shoulder becomes progressively reduced. This evolution reflects the gradual transition from strongly deformed prolate configurations toward more spherical shapes as the isotopes approach the valley of  $\beta$ -stability. For nuclei located near the valley of stability ( $^{40}\text{Ca}$  to  $^{52}\text{Ca}$ ), the ISGMR exhibits a single, well-defined main peak, providing clear evidence of spherical nuclear shapes. This behavior is particularly pronounced for the magic nuclei  $^{40}\text{Ca}$  ( $Z = 20$ ,  $N = 20$ ) and  $^{48}\text{Ca}$  ( $Z = 20$ ,  $N = 28$ ), where shell effects strongly favor spherical configurations. The theoretical predictions show good agreement with experimental data in this region, with deviations of less than 1.5 MeV for  $^{40}\text{Ca}$ , less than 3 MeV for  $^{42}\text{Ca}$  and  $^{44}\text{Ca}$ , and less than 2 MeV for  $^{48}\text{Ca}$ . However, as we move into the neutron-rich regime beyond  $^{52}\text{Ca}$ , the ISGMR structure undergoes another dramatic transformation. The previously unified main peak begins to split again, but now the fragmentation occurs predominantly on the low-energy side, creating a characteristic asymmetric profile. This low-energy splitting pattern indicates the emergence of oblate deformation in neutron-rich calcium isotopes, driven by the occupation of high-j intruder orbitals and the development of significant neutron skin effects.

On the other hand, we have systematically analyzed, in Figure 2, the isoscalar giant quadrupole resonance (ISGQR) strength distributions as a function of excitation energy across the same isotopic chain. A striking correlation emerges from these complementary calculations: the ISGQR peaks are positioned precisely at the energies corresponding to the monopole shoulders observed in the ISGMR spectra. This remarkable energy coincidence provides compelling evidence that the shoulder structures in the monopole response are not merely fragmentation artifacts, but rather arise from fundamental monopole-quadrupole coupling mechanisms. In deformed nuclei, the breaking of spherical symmetry leads to strong mixing between different multipole modes, particularly between the  $L=0$  (monopole) and  $L=2$  (quadrupole) excitations. Therefore, we can conclusively demonstrate that the rising shoulders observed in the ISGMR strength functions are the direct result of the coupling between monopole and quadrupole modes, representing a fundamental signature of nuclear deformation and collective mode mixing. This coupling becomes particularly pronounced in regions where the nuclear shape deviates significantly from sphericity, explaining why the shoulder structures are most prominent in the deformed prolate ( $^{30-34}\text{Ca}$ ) and oblate (neutron-rich) regions, while remaining suppressed in the spherical valley of stability.

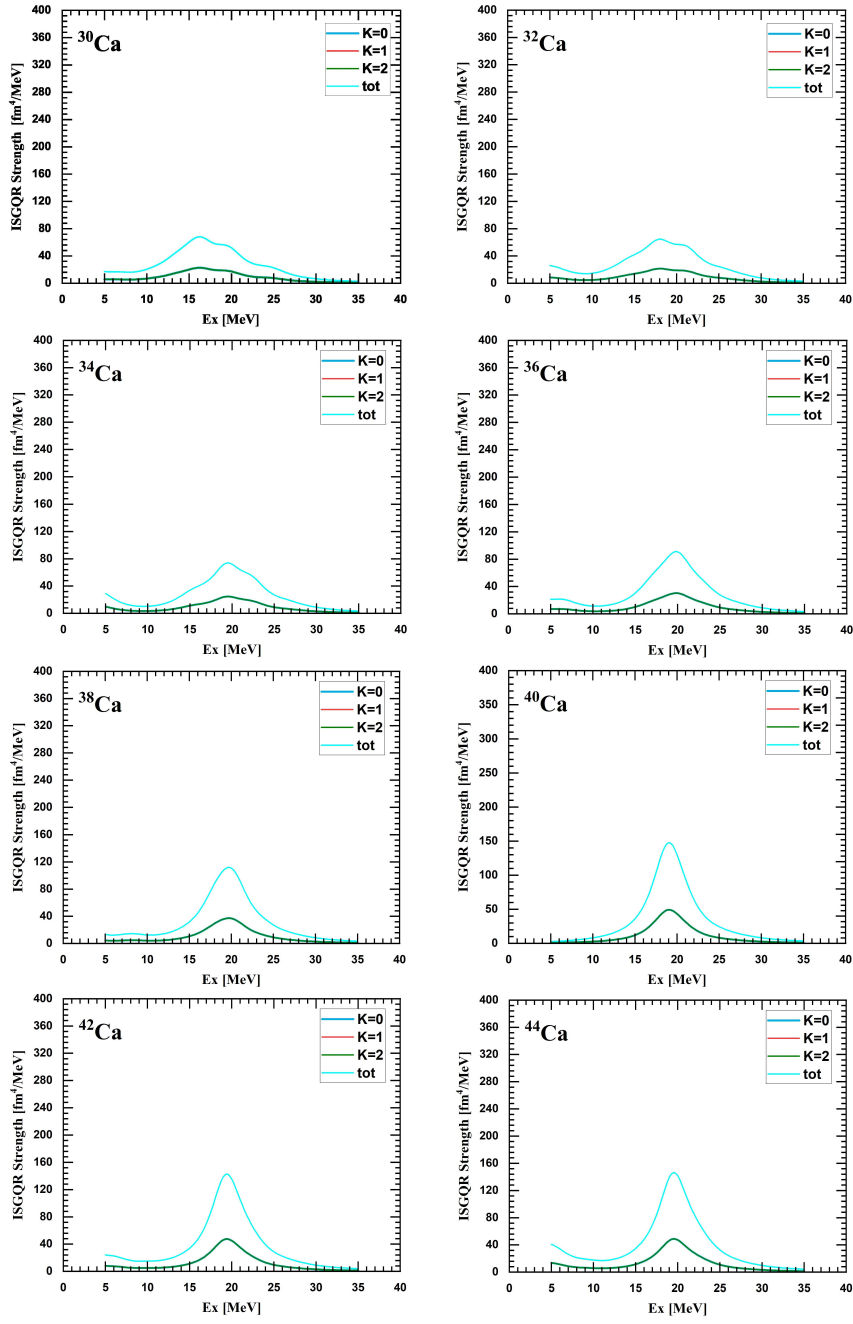


Figure 2. continued on the next page.

*Isoscalar Giant Resonances in Calcium Isotopes using CDFT and ...*

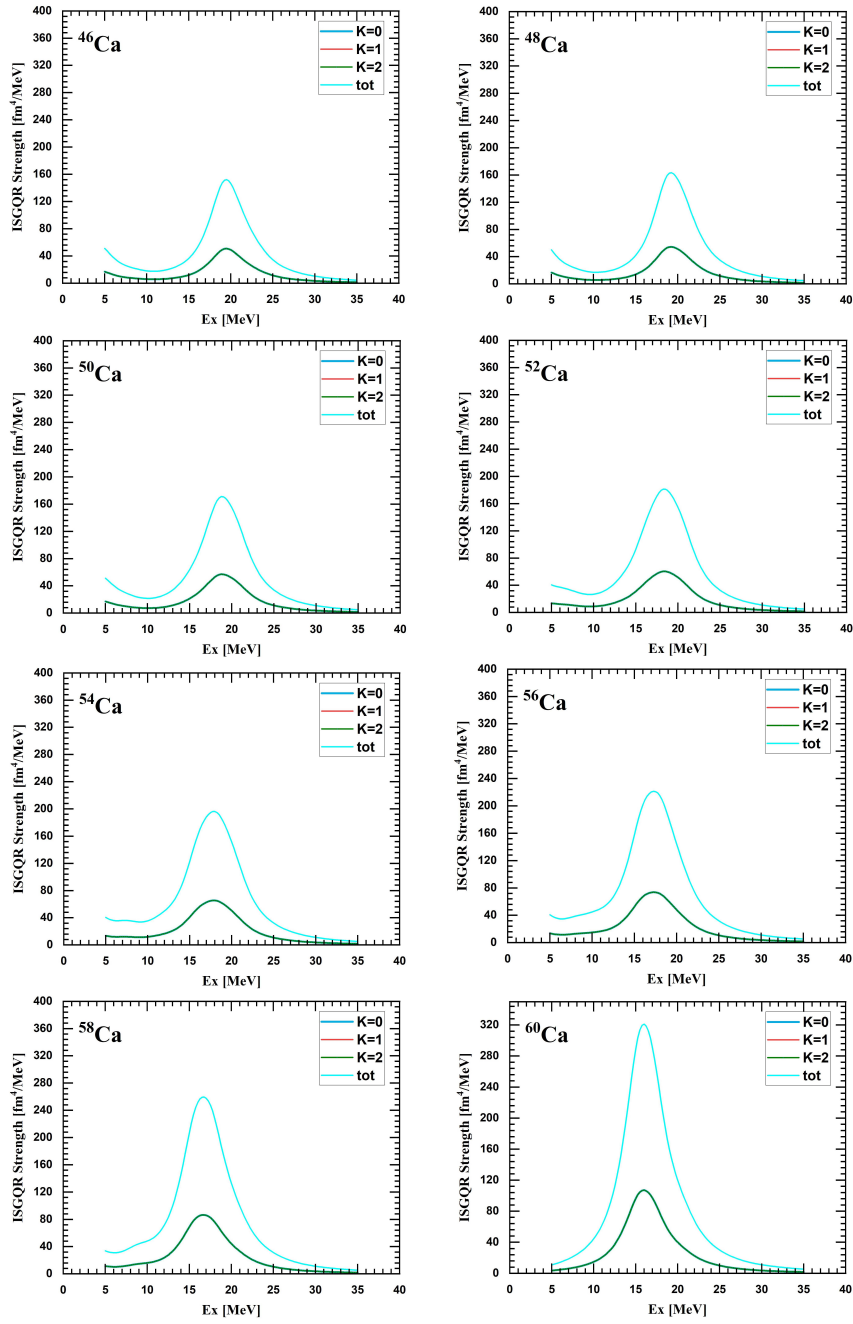


Figure 2. The calculated isoscalar quadrupole strengths in  $^{30,60}\text{Ca}$  isotopes, using DD-ME2 model.



## 4 Conclusion

This systematic investigation of isoscalar giant resonances in  $^{30,60}\text{Ca}$  isotopes using QFAM within covariant density functional theory has revealed the intimate connection between nuclear deformation and collective excitation modes. The three-phase evolution of ISGMR structure from prolate two-peak patterns through spherical single peaks to oblate low-energy splitting directly reflects the underlying shape transitions across the isotopic chain. The identification of monopole-quadrupole coupling as the mechanism driving shoulder formation represents a fundamental breakthrough in understanding collective mode interactions. Our theoretical predictions achieve excellent agreement with experimental data (deviations  $\lesssim 1.5$ -3 MeV), validating the approach and providing confidence for predictions of unmeasured neutron-rich isotopes.

## References

- [1] P.F. Bortignon, A. Bracco, R.A. Broglia, *Giant Resonances. Nuclear Structure at Finite Temperature* (CRC Press, 2019).
- [2] M. Harakeh, A. Woude, *Giant Resonances: Fundamental High-frequency Modes of Nuclear Excitation* (Oxford University Press, 2001).
- [3] G.C. Baldwin, G.S. Klaiber, *Phys. Rev.* **71** (1947) 554.
- [4] L. Donaldson, et al., *Phys. Lett. B* **776** (2018) 133.
- [5] R. Pitthan, T. Walcher, *Phys. Lett. B* **36** (1971) 563-564.
- [6] M.B. Lewis, F.E. Bertrand, *Nucl. Phys. A* **196** (1972) 337-346.
- [7] M.N. Harakeh, et al., *Phys. Rev. Lett.* **38** (1977) 676-679.
- [8] S. Fukuda, Y. Torizuka, *Phys. Rev. Lett.* **29** (1972) 1109.
- [9] B.L. Berman, S.C. Fultz, *Rev. Mod. Phys.* **47** (1972) 713.
- [10] J.P. Blaizot, et al., *Nucl. Phys. A* **591** (1995) 435.
- [11] U. Garg, G. Coló, *Prog. Part. Nucl. Phys.* **101** (2018) 95.
- [12] A. Bjelčić, and T. Nikšić, *Comp. Phys. Commun.* **253** (2020) 107184.
- [13] M. El Adri, M. Oulne, *Eur. Phys. J. Plus* **135** (2020) 268.
- [14] M. El Adri, M. Oulne, *IJMPE* **29** (2020) 2050089.
- [15] G.A. Lalazissis, T. Nikšić, D. Vretenar, P. Ring, *Phys. Rev. C* **71** (2005) 024312.
- [16] Y. Tian, Z.Y. Ma, P. Ring, *Phys. Rev. Lett. B* **676** (2009) 44-50.